

# Nucleation of deformation twins in nanocrystalline face-centered-cubic metals processed by severe plastic deformation

Y. T. Zhu<sup>a)</sup>

*Los Alamos National Laboratory, Los Alamos, New Mexico 87545*

X. Z. Liao

*Los Alamos National Laboratory, Los Alamos, New Mexico 87545*

*and The University of Chicago/Argonne National Laboratory Consortium for Nanoscience Research, University of Chicago, Illinois 60637*

S. G. Srinivasan

*Los Alamos National Laboratory, Los Alamos, New Mexico 87545*

E. J. Lavernia

*University of California, Davis, California 95616*

(Received 25 May 2005; accepted 28 June 2005; published online 15 August 2005)

Nanocrystalline (nc) materials are known to deform via mechanisms not accessible to their coarse-grained counterparts. For example, deformation twins and partial dislocations emitted from grain boundaries have been observed in nc Al and Cu synthesized by severe plastic deformation (SPD). This paper further develops an earlier dislocation-based model on the nucleation of deformation twins in nc face-centered-cubic (fcc) metals. It is found that there exists an optimum grain-size range in which deformation twins nucleate most readily. The critical twinning stress is found determined primarily by the stacking fault energy while the optimum grain size is largely determined by ratio of shear modulus to stacking fault energy. This model formulated herein is applicable to fcc nanomaterials synthesized by SPD techniques and provide a lower bound to the critical twinning stress. © 2005 American Institute of Physics. [DOI: 10.1063/1.2006974]

## I. INTRODUCTION

Nanocrystalline (nc) metals are solids with grain sizes smaller than 100 nm. They typically exhibit mechanical properties that are markedly superior to those of conventional materials. For example, they have been reported to have excellent superplasticity,<sup>1</sup> high strength,<sup>2–6</sup> and in a few cases a combination of high strength and excellent ductility.<sup>2,5</sup> These exceptional properties are attributed in part to their unique deformation mechanisms, which are derived from their unusual microstructures.<sup>7</sup>

Our current understanding of the deformation mechanisms in nc metals has accrued mostly from molecular-dynamics (MD) simulations.<sup>8–13</sup> Such simulations predict nc metals to deform *via* grain boundary (GB) sliding at very fine grain sizes (e.g., 3–10 nm).<sup>9,10</sup> In practice, this prediction will be affected by the structure of the grain boundaries, which strongly depends on processing history. Partial dislocation emission from GBs (Ref. 8) is shown to dominate at several tens of nanometers. Deformation twins (DTs) have been predicted in nc Al,<sup>8,12</sup> Ni,<sup>10,11</sup> and Cu.<sup>14</sup> DTs and partial dislocation emissions from GBs were recently verified in nc Al, Cu, and Pd by high-resolution transmission electron microscopy.<sup>7,15–19</sup>

Al in its coarse-grained state has never been observed to deform by twinning, except at crack tips,<sup>20</sup> because of its very high stacking fault energy (SFE). Coarse-grained copper

does not deform by twinning<sup>21,22</sup> except at very high strain rates<sup>23,24</sup> and/or low temperatures.<sup>25</sup> Moreover, in coarse-grained Cu smaller grain size was found to impede deformation twinning, which is also true for many other metals.<sup>26,27</sup> In contrast, twinning becomes a major deformation mechanism in nc Cu processed by high-pressure torsion (HPT) at room temperature and a low strain rate.<sup>17</sup> In addition, it was also found that under the same HPT condition, twinning only occurred in crystalline domains that are smaller than 50 nm.<sup>28</sup> These results indicate that the nc materials indeed deform via mechanisms not accessible to their coarse-grained counterparts and grain size plays a critical role in the formation of DTs.

The nucleation and growth of DTs in nc materials are not well-understood phenomena. Both atomistic simulations and experimental studies indicate that DTs are formed by partial dislocation emissions from GBs.<sup>8,14,15,17,19,29</sup> However, it is not clear under what conditions DTs will nucleate and grow. For example, atomistic simulations do not predict what critical stress is needed for DT nucleation and growth or what grain size is optimum for DT nucleation. Recently, Frøseth *et al.*<sup>30</sup> argued that it is much more difficult for a twin to nucleate than for it to grow basing on the nucleation barriers of various partials as described by the generalized planar fault energy curves. However, their analysis is only qualitative and does not provide a critical stress or grain size for twin nucleation. Another problem with MD simulations<sup>8–10</sup> is that they usually use extremely high strain rates in the order of  $10^6$ – $10^8$  s<sup>-1</sup>, which correspond to explosive deformation in a real experiment. Since it is well established that the strain

<sup>a)</sup>Author to whom correspondence should be addressed; electronic mail: yzhu@lanl.gov

rate significantly affects the deformation mechanisms of materials,<sup>7,17</sup> the interpretation of the atomistic simulation results is rendered complex. Accordingly, it is of interest to study the grain-size effect on the deformation twinning without the complications that are associated with high strain rates.

Two similar analytical models were proposed to explain the formation of DTs in nc metals.<sup>18,31</sup> The models are based on dislocation mechanisms in coarse-grained materials. They describe a slower critical stress increase with decreasing grain size for moving twinning partials than for moving lattice dislocations. This leads to deformation twinning below a critical grain size. Unfortunately, experimental data show that for coarse-grained metals the critical stress for twinning actually increases faster with decreasing grain size than that for lattice dislocation in many metals and alloys including Cu and Al.<sup>26</sup> Therefore, the aforementioned models are not supported by the experimental data in coarse-grained metals, let alone nc metals. The problem with these two models is that they are not based on sound deformation physics of nanometals.

A more recent analytical dislocation model by Asaro *et al.*<sup>32</sup> predicts that below a certain critical grain size in nc metals, partial dislocations from GBs need a lower stress to move than lattice dislocations. The model of Asaro *et al.* predicts a realistic, low twinning stress that is obtainable under experimental conditions such as ball milling. However, the model fails to address two critical issues. First, the emission of a partial dislocation does not guarantee the nucleation of a DT because a trailing partial could follow to erase the stacking fault formed by the first partial. Second, random emissions of partial dislocations from a GB would give a DT equal probability to grow or to shrink, which cannot explain the DT growth and the observed large DTs in nc Al and Cu.<sup>15,17</sup>

To address the above two issues, we recently developed a preliminary analytical model to describe the nucleation and growth of DTs in nc Al.<sup>33</sup> This model describes the critical stresses required for moving lattice dislocations and various partial dislocations, and predicts an optimum grain size and a critical external stress for twin nucleation. In addition, it revealed a stress-controlled twin growth mechanisms, which explains why and how a twin can grow in the absence of the conventional pole mechanism. Our model could explain very well the experimental observations of DTs in nc Al synthesized by cryogenic milling.<sup>15,33</sup> However, in its original form the model is difficult to use and requires extensive effort to compute and compare various stresses. In this paper we shall further develop and simplify this model and examine its validity with more experimental data. We shall also examine the effect of SFE and shear modulus on the critical stress and optimum grain size for DT nucleation.

## II. MODEL DEVELOPMENT

To understand the nucleation mechanisms of DTs in nc fcc metals, we draw on the simulation results<sup>11,12</sup> and experimental observations<sup>17,18</sup> that Shockley partial dislocations are emitted from GBs. One scenario of dislocation emission

from GBs is that a dislocation is nucleated on a GB and then moves into a grain interior under an external stress. Basing on theoretical models of dislocation emissions from crack tips,<sup>34,35</sup> Van Swygenhoven *et al.*<sup>30,36</sup> argued that the generalized planar fault energies curves should be used for the nucleation of partial dislocations from GBs. However, they did not give quantitative results or analytical description on how this be accomplished.

Another scenario is that nongeometrically necessary lattice dislocations at a GB or a crystalline domain boundary simply dissociate into two partials and one of partials move into the grain interior under an external stress, thus avoiding the requirement for nucleation of partial dislocations. Such a scenario exists in nc materials synthesized by severe plastic deformation techniques.<sup>28,31,37</sup> For example, high density of dislocations were found on the twin domain boundaries in nc Cu synthesized by HPT (see Fig. 1),<sup>28</sup> strongly supporting this scenario. Furthermore, in this scenario the emission of partial dislocations does not need to overcome the energy barrier, e.g., the unstable stacking fault energy or the unstable twin fault energy, described in the generalized planar fault energy curve. Therefore, only the SFE is relevant and need to be considered.

In our model we shall only consider the latter scenario. Importantly, our recent model<sup>33</sup> predicted that DTs were formed in two steps: (1) formation of a stacking fault across the whole grain by dissociation of a lattice dislocation, and (2) emission of a twinning partial on a slip plane adjacent to the stacking fault plane. These two steps are consistent with the scenario considered here. In the following we shall further develop and simplify this model.

We use some of the assumptions used in a previous model for partial dislocation emissions:<sup>32,33</sup> (1) a grain with a square (111) slip plane is considered for simplicity, and (2) partial dislocations are formed by dissociation of lattice dislocations, thus avoiding their nucleation from GBs. In addition, we shall ignore the Peierls stress because it is very small (e.g., <1 MPa for Al).<sup>33</sup> We also ignore the differences in the core energies between partial and lattice dislocations because our calculations show their effects to be negligible.

As shown in Fig. 2(a), under an external shear stress, a leading Shockley partial dislocation,  $\mathbf{b}_1 = a/6[2\bar{1}\bar{1}]$ , is emitted from grain boundary  $AB$  (see the line  $AabB$ ). Note that dislocation emission from a GB referred to in this model does not include the process of dislocation nucleation because we are only dealing with the scenario in which dislocations already exist on the grain boundary (see Fig. 1).<sup>28,37</sup> This partial dislocation  $\mathbf{b}_1$  is pinned at the triple junctions  $A$  and  $B$  so that two segments of partial dislocation lines ( $Aa$  and  $Bb$ ) are deposited on GBs. Similarly, a trailing Shockley partial dislocation,  $\mathbf{b}_2 = a/6[1\bar{2}1]$ , is emitted from grain boundary  $AB$  and forms the  $Aa'b'B$  dislocation line. Partial dislocation lines  $ab$  and  $a'b'$  are separated by a stacking fault, and they would form a screw dislocation  $a/2[1\bar{1}0]$  if collapsed together. The two partial dislocations react to form two lattice edge dislocation segments,  $Aa'$  and  $Bb'$ , at the grain boundaries. Note that the partial segments  $ab$  and  $a'b'$

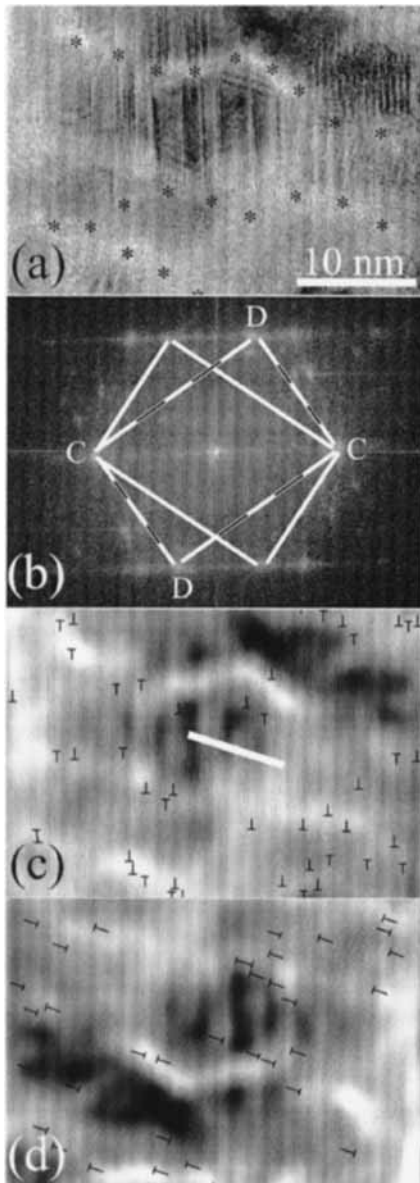


FIG. 1. (a) A  $\langle 110 \rangle$  HREM image of elongated nanodomains in HPT-processed Cu. The domain boundaries are highlighted using black asterisks. (b) Fourier transformation of (a). Two sets of lattice forming a twin relationship are indicated by two rectangles. (c) Inverse Fourier transformation using the (000) and two spots marked "C" in (b). Dislocation cores are marked with black "T" and their slip plane is indicated using a white straight line. (d) Inverse Fourier transformation using the (000) and two spots marked "D" in (b).

will be curved in a real situation. Here we assume them to be straight lines to simplify the mathematics without sacrificing the physics.

The partial dislocation system in Fig. 2(a) is identical to a screw dislocation,  $a/2[1\bar{1}0]$ , that is dissociated into two partials. Therefore, we call it a *screw system* hereafter. Two other possible dislocation systems also exist. In Fig. 2(a), if a  $90^\circ$  partial,  $\mathbf{b}_1 = a/6[11\bar{2}]$ , is leading, and the  $30^\circ$  partial,  $\mathbf{b}_2 = a/6[2\bar{1}\bar{1}]$ , is trailing, the dislocation system is called the  $60^\circ$  I system. On the other hand, if  $30^\circ$  partial is leading and

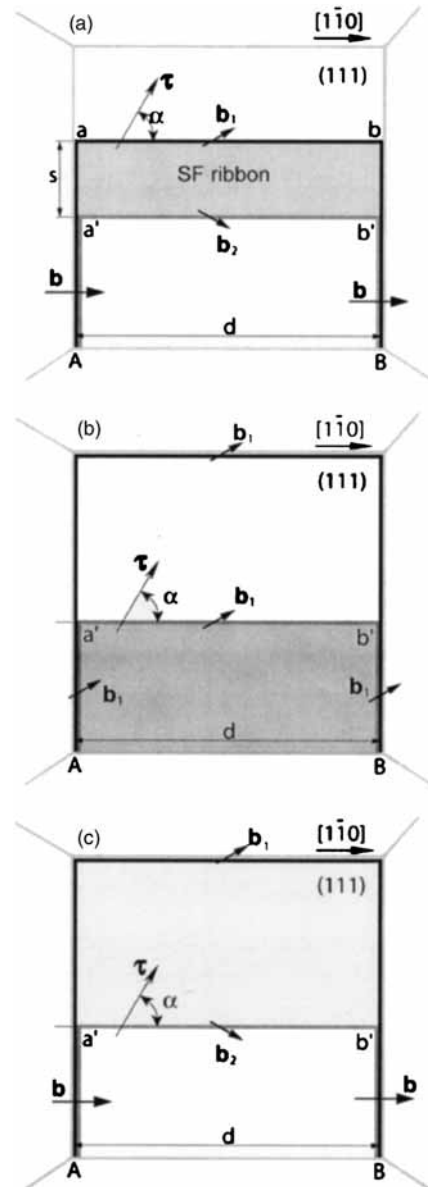


FIG. 2. A schematic illustration of the dislocation model for the nucleation of deformation twins. (a) a lattice screw dislocation dissociated into two partials  $\mathbf{b}_1$  and  $\mathbf{b}_2$ ; (b) the nucleation of a deformation twin via the emission of a twinning partial on a (111) plane adjacent to the stacking fault plane; and (c) the emission of a trailing partial that removes the stacking fault.

the  $90^\circ$  partial is trailing, the resulting dislocation system is called the  $60^\circ$  II system. The  $60^\circ$  I system was analyzed in our earlier paper<sup>33</sup> and we shall directly use its results. The  $60^\circ$  II system is not operational<sup>33</sup> and therefore will not be analyzed here.

### A. Screw system

In this section, we shall analyze the screw system in detail. The first step to nucleate a DT is to create a stacking fault that extends from a GB into the grain interior or across the whole grain. This can be accomplished by two possible ways. The first is to emit a  $30^\circ$  partial dislocation  $\mathbf{b}_1$  at grain boundary AB [see Fig. 2(a)], and the second is to have the

stacking fault ribbon [Fig. 2(a)] stretch all the way across the grain so that the trailing partial stays pinned at the grain boundary  $AB$ . As found in our earlier work,<sup>33</sup> both scenarios are possible depending on the orientation  $\alpha$  of the external stress  $\tau$ . However, the second scenario needs lower external stress to activate and thus determines the critical twinning stress. In the following we shall first derive stresses needed for activating various partial dislocations as well as the lattice screw dislocation as a function of grain size and stress orientation. These equations will then be used to further derive equations for determining the critical twinning stress and optimum grain size for twin nucleation.

In Fig. 2(a), if the second partial dislocation  $\mathbf{b}_2$  is not emitted, the partial dislocation  $\mathbf{b}_1$  will create a stacking fault in its wake as it moves across the (111) slip plane. For the partial dislocation segment  $ab$  to move a distance  $\Delta x$ , the work done by  $\tau$  can be expressed as

$$\Delta E_c = \Delta x d \tau \cdot \mathbf{b}_1 = \Delta x d \tau b_1 \cos(\alpha - 30^\circ), \quad (1)$$

where  $b_1$  is the absolute length of  $\mathbf{b}_1$ ,  $d$  is the grain size defined in Fig. 2(a), and  $30^\circ$  is the angle between  $\mathbf{b}_1$  and dislocation line  $ab$ . The stacking fault energy increase is

$$\Delta E_\gamma = \Delta x d \gamma, \quad (2)$$

where  $\gamma$  is the SFE per unit area. The increased dislocation line energy (ignoring the dislocation core energy) is

$$\Delta E_d = 2 \Delta s \frac{G b_1^2 (1 - \nu \cos^2 60^\circ)}{4\pi(1 - \nu)} \ln \frac{R}{r_0}, \quad (3)$$

where  $G$  is the shear modulus,  $\nu$  is Poisson's ratio,  $R$  can be approximated as the grain size  $d$ , and  $r_0$  is approximated as  $b$ , the magnitude of a lattice dislocation. For fcc metals,  $b = a/\sqrt{2}$  and  $b_1 = a/\sqrt{6}$ , where  $a$  is the lattice parameter.

The external shear stress  $\tau$  has to overcome the SFE and the energy increase associated with the lengthening of dislocation segments  $Aa$  and  $Bb$ . In other words, work done by  $\tau$  on partial segment  $ab$  equals the sum of SFE increase and dislocation energy increase,<sup>38,39</sup> i.e.,

$$\Delta E_\tau = \Delta E_\gamma + \Delta E_d. \quad (4)$$

Substituting Eqs. (1)–(3) into Eq. (4) and simplifying, it yields

$$\tau_p = \frac{1}{\cos(\alpha - 30^\circ)} \left[ \frac{\sqrt{6}\gamma}{a} + \frac{Ga(4 - \nu)}{8\sqrt{6}\pi(1 - \nu)d} \ln \frac{\sqrt{2}d}{a} \right], \quad (5)$$

where  $\tau_p$  is the critical external shear stress to move partial  $\mathbf{b}_1$ .

For the stacking fault ribbon in Fig. 2(a) to move forward,  $\tau$  needs to overcome the energy increase associated with the lengthening of lattice dislocation segments  $Aa'$  and  $Bb'$ . This is equivalent to moving a lattice screw dislocation irrespective of the existence of the stacking fault ribbon. However, the stacking fault area will not change. Following the procedure used for deriving Eq. (5), we obtain the critical shear stress for moving a lattice screw dislocation as

$$\tau_L = \frac{Ga}{2\sqrt{2}\pi(1 - \nu)d \cos \alpha} \ln \frac{\sqrt{2}d}{a}. \quad (6)$$

The partial dislocation and the lattice dislocation compete with each other, and the one requiring a lower stress will prevail.

As shown in Fig. 2(a), the partials  $\mathbf{b}_1$  and  $\mathbf{b}_2$  have different orientations, indicating that they will be subjected to different driving forces under an external shear stress  $\tau$ . This difference will affect the width of the stacking fault ribbon in the same way as changing the SFE would. Also, the partial dislocations form lattice dislocation segments along  $Aa'$  and  $Bb'$ , which have higher energy than partial dislocations. Therefore, the lattice dislocation segments will exert a drag on partial dislocation segments  $a'b'$ , which is equivalent to reducing the SFE. The apparent SFE per unit area can be calculated from the above analysis as<sup>16</sup>

$$\gamma_a = \gamma - \tau \cdot (\mathbf{b}_1 - \mathbf{b}_2) - \frac{2}{d} \left[ \frac{Gb^2}{4\pi(1 - \nu)} \ln \frac{R}{r_0} - \frac{Gb_1^2(1 - \nu \cos^2 60^\circ)}{4\pi(1 - \nu)} \ln \frac{R}{r_0} \right]. \quad (7)$$

Simplifying Eq. (7) yields

$$\gamma_a = \gamma - \frac{Ga^2(8 + \nu)}{48\pi(1 - \nu)d} \ln \frac{\sqrt{2}d}{a} - \frac{\tau a \sin \alpha}{\sqrt{6}}. \quad (8)$$

The stacking fault width is inversely proportional to SFE, i.e.,  $s/s_0 = \gamma/\gamma_a$ , where  $s$  is the stacking fault width in nanograins under external stress and  $s_0$  is the intrinsic stacking fault width of a screw dislocation. Therefore, when the stacking fault ribbon in Fig. 1(a) moves under an external shear stress  $\tau$ , the stacking fault width  $s$  can be described as

$$s_\tau = \frac{\gamma s_0}{\gamma - Ga^2(8 + \nu)/[48\pi(1 - \nu)d] \ln \sqrt{2}d/a - \tau a \sin \alpha / \sqrt{6}}. \quad (9)$$

For a screw dislocation,  $s_0$  can be described as<sup>38,39</sup>

$$s_0 = \frac{Gb_1^2 2 - 3\nu}{8\pi\gamma 1 - \nu}. \quad (10)$$

Setting  $s_\tau = d$ , we can determine the critical external shear stress  $\tau$  above which a stacking fault across the whole grain is generated. Equation (9) can be used to determine if a stacking fault spreads across a whole grain under an external shear stress.

For a twin to nucleate, a second  $30^\circ$  leading partial dislocation with the same Burgers vector as  $\mathbf{b}_1$  needs to emit from the GB on a slip plane adjacent to the first stacking fault [see Fig. 2(b)]. We define this partial dislocation as the twinning partial and the stress to move it as the twinning stress  $\tau_{\text{twin}}$ . There is also a high possibility that a trailing partial  $\mathbf{b}_2$  will emit on the stacking fault plane and consequently erase the stacking fault as it moves across the plane. The trailing partial requires a shear stress  $\tau_{\text{trail}}$  to move. The twinning partial needs to compete with the trailing partial to nucleate a twin.

As the twinning partial moves forward, it generates a two-layer twin nucleus, and the stacking fault is replaced with two twin boundaries. Since the energy of a twin boundary is about half the SFE,<sup>39</sup> the external shear stress  $\tau$  only

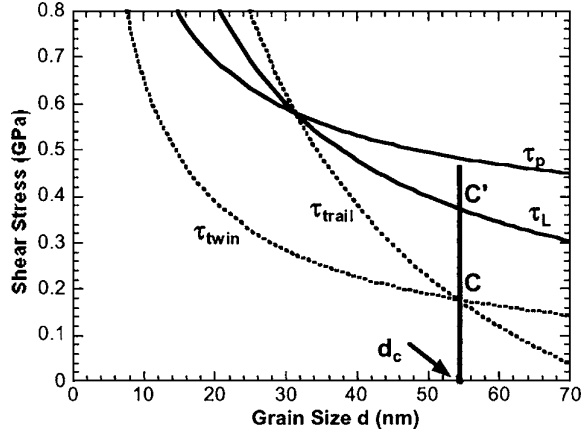


FIG. 3. The critical stresses  $\tau_p$ ,  $\tau_L$ ,  $\tau_{\text{twin}}$ , and  $\tau_{\text{trail}}$  as a function of grain size  $d$  for  $\alpha=26.5^\circ$  in nc Cu.

needs to overcome the length increase of partial dislocation segments  $Aa'$  and  $Bb'$  [see Fig. 2(b)]. Following the procedure for the derivation of  $\tau_p$  in Eq. (5), we can derive the critical twinning stress as

$$\tau_{\text{twin}} = \frac{Ga(4-\nu)}{8\sqrt{6}\pi(1-\nu)d \cos(\alpha-30^\circ)} \ln \frac{\sqrt{2}d}{a}. \quad (11)$$

The trailing partial  $a'b'$ , with a Burgers vector of  $\mathbf{b}_2$  is driven by both the external shear stress  $\tau$  and the reduction of total SFE [see Fig. 2(c)]. However, lattice dislocation segments  $Aa'$  and  $Bb'$  are also generated on the GB, and exert a drag force. Considering these factors, stress needed to move the trailing partial can be derived as

$$\tau_{\text{trail}} = \frac{1}{\cos(\alpha+30^\circ)} \left[ \frac{\sqrt{6}(8+\nu)Ga}{48\pi(1-\nu)d} \ln \frac{\sqrt{2}d}{a} - \frac{\sqrt{6}\gamma}{a} \right]. \quad (12)$$

To nucleate a DT, the twinning partial needs to prevail over the trailing partial, i.e.,  $\tau_{\text{twin}} < \tau_{\text{trail}}$ .

In our previous work,<sup>33</sup> we found that the curve of critical twinning stress versus grain size follows a cup and handle shape. It is in the cup section that there exists an optimum grain size at which the twinning stress is the lowest. To determine this critical grain size and the lowest twinning stress, we draw from our previous work<sup>33</sup> the following useful results: (1) Only the cup section needs to be considered; (2) For each dislocation system, the cup section corresponds to a certain stress orientation range, i.e., for the screw system,  $-30^\circ < \alpha < 60^\circ$ , and for the  $60^\circ$  I System,  $30^\circ < \alpha < 120^\circ$ ; (3) In this cup section, the stacking fault prior to twin nucleation is formed by the spreading of the stacking fault ribbon of a dissociated lattice dislocation across the whole grain.

To assist with understanding the relationship among  $\tau_p$ ,  $\tau_L$ ,  $\tau_{\text{twin}}$ , and  $\tau_{\text{trail}}$ , we plot them in Fig. 3 [Eqs. (5), (6), (11), and (12)] as a function of grain size  $d$  at a shear stress orientation angle  $\alpha=26.5^\circ$  using the data for Cu in Table I. This  $\alpha$  angle is chosen because, as shown later, it is the angle at which the twinning stress is the lowest. Figure 3 is typical for the screw system in the stress orientation range of  $-30^\circ < \alpha < 60^\circ$ . Close examination of  $\tau_{\text{twin}}$  and  $\tau_{\text{trail}}$  curves in Fig. 3 reveals a critical grain size  $d_c$  below which  $\tau_{\text{twin}} < \tau_{\text{trail}}$ . In other words,  $d_c$  represents a critical grain size below which a twin would nucleate. Setting  $\tau_{\text{twin}} = \tau_{\text{trail}}$  and substituting  $\tau_{\text{twin}}$  and  $\tau_{\text{trail}}$  with Eqs. (11) and (12), we obtain

$$\frac{1}{d_c} \ln \frac{\sqrt{2}d_c}{a} = \frac{\gamma}{Ga^2(8+\nu)\cos(\alpha-30^\circ) - (4-\nu)\cos(\alpha+30^\circ)}. \quad (13)$$

Equation (13) indicates that the critical grain size  $d_c$  is a function of external shear stress orientation  $\alpha$ .

Figure 3 shows that  $\tau_{\text{twin}}$  and  $\tau_{\text{trail}}$  cross each other at point C. However, the stress magnitude at point C cannot nucleate a DT, because the precondition of the DT nucleation is to first form a stacking fault. As shown, at grain size  $d_c$ ,  $\tau_L < \tau_p$ , i.e., the lattice dislocation, not the partial dislocation, is operating.  $\tau_L$  can be found as 0.375 GPa at point C'. Under such an external stress, the stacking fault width calculated using Eq. (9) is much larger than  $d_c$ , which means that a stacking fault is first generated by the wide stacking fault ribbon of a lattice screw dislocation and then a DT is nucleated. Therefore, the critical twin nucleation stress at a given  $\alpha$  is determined by point C' in Fig. 3. This critical stress can be calculated by substituting Eq. (13) into Eq. (6), which yields

$$\tau_c = \frac{\gamma}{a} f(\alpha), \quad (14)$$

where

$$f(\alpha) = \frac{12\sqrt{2} \cos(\alpha-30^\circ)}{\cos \alpha [(8+\nu)\cos(\alpha-30^\circ) - (4-\nu)\cos(\alpha+30^\circ)]}. \quad (15)$$

It is obvious that the critical twin nucleation stress  $\tau_c$  is a function of shear stress orientation  $\alpha$ . The lowest twin nucleation stress can be determined by finding the minimum  $f(\alpha)$  value from Eq. (15). For a given  $\nu$  value, we can set  $df(\alpha)/d\alpha=0$  and solve for the optimum  $\alpha_{\text{op}}$  at which  $f(\alpha)$  is at its minimum. For most fcc metals and alloys, Poisson's ratio  $\nu$  ranges from 0.27 to 0.44.<sup>40</sup> Our calculations show that  $\alpha_{\text{op}}$  value varies from  $27.3^\circ$  to  $25.7^\circ$  (see Fig. 4), i.e., the  $\alpha_{\text{op}}$

TABLE I. Parameters for Cu and Al used in our model (see Refs. 39 and 42).

	$G$ (GPa)	$\nu$	$\gamma$ (mJ/m <sup>2</sup> )	$a$ (Å)	$\tau_{\text{min}}$ (GPa)	$d_{\text{op}}$ (nm)
Al	26.5	0.345	122	4.04	0.88–0.91	4.9–7.4
Cu	54.6	0.343	45	3.6146	0.36–0.37	38.4–54.2

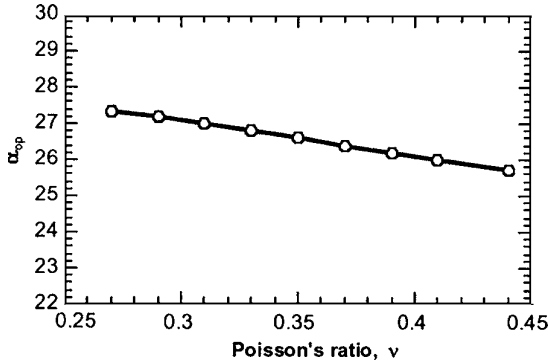


FIG. 4. Variation of the optimum orientation angle  $\alpha_{op}$  with Poisson's ratio for the screw system.

value is insensitive to the variation of  $\nu$  value. For simplicity, we can approximate  $\alpha_{op}=26.5^\circ$  irrespective  $\nu$  value, and can calculate the minimum  $f(\alpha)$  value from Eq. (15) as

$$f(\alpha)_{\min} = \frac{12.211}{3.727 + \nu}. \quad (16)$$

Our calculation indicates that error from Eq. (16) due to the approximation of  $\alpha_{op}$  is less than 0.03% when  $\nu$  is varied from 0.27 to 0.44. Substituting Eq. (16) into Eq. (14) yield the minimum stress for twin nucleation from a screw system as

$$\tau_{\min} = \frac{12.211}{3.727 + \nu} \frac{\gamma}{a}. \quad (17)$$

Similarly, Eq. (13) can be simplified by the approximation of  $\alpha_{op}=26.5^\circ$  as

$$\frac{d_{op}}{\ln(\sqrt{2}d_{op}/a)} = \frac{3.727 + \nu}{97.053(1 - \nu)} \frac{Ga^2}{\gamma}, \quad (18)$$

where  $d_{op}$  is the optimum grain size at which  $f(\alpha)$  is at its minimum. Our calculation shows that the error caused by the approximation on the right side of Eq. (18) is less than 0.7%.

Therefore, for the screw system the minimum twin nucleation stress can be calculated from Eq. (17), while optimum grain size for twin nucleation can be determined by solving Eq. (18).

### B. The $60^\circ$ I System

We can also derive the optimum stress orientation  $\alpha_{op}$ , the minimum twinning stress  $\tau_{\min}$ , and the optimum grain size  $d_{op}$  for the  $60^\circ$  I System. The starting equations for such derivation, i.e.,  $\tau_P$ ,  $\tau_L$ ,  $\tau_{\text{twin}}$ , and  $\tau_{\text{trail}}$ , have already been derived:<sup>33</sup>

$$\tau_P = \frac{1}{\sin \alpha} \left( \frac{\sqrt{6}\gamma}{a} + \frac{Ga}{2\sqrt{6}\pi d} \ln \frac{\sqrt{2}d}{a} \right), \quad (19)$$

$$\tau_L = \frac{Ga(4 - 3\nu)}{8\sqrt{2}\pi(1 - \nu)d \cos(\alpha - 60^\circ)} \ln \frac{\sqrt{2}d}{a}, \quad (20)$$

$$\tau_{\text{twin}} = \frac{Ga}{2\sqrt{6}\pi d \sin \alpha} \ln \frac{\sqrt{2}d}{a}, \quad (21)$$

$$\tau_{\text{trail}} = \frac{\sqrt{6}}{\cos(\alpha - 30^\circ)} \left[ \frac{Ga(8 - 5\nu)}{48\pi(1 - \nu)d} \ln \frac{\sqrt{2}d}{a} - \frac{\gamma}{a} \right]. \quad (22)$$

Following the procedure for the screw system, we first set  $\tau_{\text{twin}} = \tau_{\text{trail}}$ , which yields

$$\frac{1}{d_c} \ln \frac{\sqrt{2}d_c}{a} = \frac{\gamma}{Ga^2(8 - 5\nu)\sin \alpha - 4(1 - \nu)\cos(\alpha - 30^\circ)}. \quad (23)$$

Substituting Eq. (23) into Eq. (20) yields

$$\tau_c = \frac{\gamma}{a \cos(\alpha - 60^\circ)} \frac{3\sqrt{2}(4 - 3\nu)\sin \alpha}{[(8 - 5\nu)\sin \alpha - 4(1 - \nu)\cos(\alpha - 30^\circ)]}. \quad (24)$$

Setting  $d\tau_c/d\alpha=0$ , we can obtain the optimum  $\alpha_{op}$  at which  $\tau_c$  is at its minimum. Similar to the screw system,  $\alpha_{op}$  can be approximated as  $85.2^\circ$ , irrespective the  $\nu$  value. Substituting  $\alpha_{op}=85.2^\circ$  into Eq. (24) yields

$$\tau_{\min} = \frac{1.715(4 - 3\nu)}{2.089 - \nu} \frac{\gamma}{a}. \quad (25)$$

Substituting  $\alpha_{op}=85.2^\circ$  into Eq. (23) yields

$$\frac{d_{op}}{\ln(\sqrt{2}d_{op}/a)} = \frac{2.089 - \nu}{54.985(1 - \nu)} \frac{Ga^2}{\gamma}. \quad (26)$$

Our calculations show that the approximation of  $\alpha_{op}=85.5^\circ$  led to an error of  $<0.2\%$  in  $\tau_{\min}$ , and an error of  $<1.2\%$  in the right side of Eq. (26). Therefore, for the  $60^\circ$  I system, the minimum twin nucleation stress can be calculated from Eq. (25), while optimum grain size for twin nucleation can be determined by solving Eq. (26).

## III. DISCUSSIONS

### A. Effect of stacking fault energy and shear modulus

As shown in our calculation later and in our previous work, the  $60^\circ$  I system twins at a slightly lower stress and smaller optimum grain size<sup>33</sup> than the screw system. In a real grain, the dislocation is most likely a mixed nature, and the twin nucleation stress and optimal grain size are between those of the  $60^\circ$  I system and the screw system, i.e.,

$$\frac{1.715(4 - 3\nu)}{2.089 - \nu} \frac{\gamma}{a} \leq \tau_{\min} \leq \frac{12.211}{3.727 + \nu} \frac{\gamma}{a}, \quad (27)$$

$$\frac{2.089 - \nu}{54.985(1 - \nu)} \frac{Ga^2}{\gamma} \leq \frac{d_{op}}{\ln(\sqrt{2}d_{op}/a)} \leq \frac{3.727 + \nu}{97.053(1 - \nu)} \frac{Ga^2}{\gamma}. \quad (28)$$

For fcc metals and alloys, neither Poisson's ratio  $\nu$  nor lattice parameter changes dramatically from material to material. However, the SFE  $\gamma$  could vary by more an order of magnitude. In addition, the slight change in alloy composition could significantly change the SFE.<sup>41</sup> Therefore, it is reasonable to say from Eq. (27) that the minimum twin

nucleation stress for both the screw system and the  $60^\circ$  I system are largely determined by the SFE. Lower SFE leads to lower twin nucleation stress.

Equation (28) indicates that the optimum grain size for twin nucleation is largely determined by the ratio of shear modulus to SFE ( $G/\gamma$ ). Higher shear modulus and lower SFE leads to larger optimum grain size for twin nucleation.

## B. Application to nanocrystalline Cu and Al

Nanocrystalline Cu and Al have been studied more extensively than other nc metals<sup>8–18</sup> and have more experimental data to compare with our model. Parameters for Cu and Al used in our model as well as the ranges of minimum twinning stress and optimum grain sizes calculated using Eqs. (27) and (28) are listed in Table I. First, we note that the minimum stresses and optimum grain sizes for twin nucleation in Table I agree very well with our earlier paper,<sup>33</sup> attesting to the accuracy of Eqs. (27) and (28). Second, we can see that nc Cu can form DTs at significantly lower stresses and larger grain sizes than Al.

As listed in Table I, in nc Al the optimum grain size for DT nucleation is in the range of 4.9–7.4 nm. However, atomistic simulations predicted GB sliding as the primary deformation mode in nc Ni (Ref. 43) and nc Cu (Ref. 14) when their grain sizes are below 10 nm. Such a trend also likely exists in nc Al, but again, this behavior will be affected by processing history. In other words, GB sliding, instead of deformation twinning, is the likely deformation mode in nc Al with grain sizes smaller than 10 nm. Indeed, DTs were not observed in grains smaller than 10 nm in a nc Al produced by cryogenic ball milling.<sup>7,15</sup> Twins were only observed at small corners of grains of several tens nanometers.<sup>15</sup> Such a large grain is too large for GB sliding, but its small corners can nucleate DTs at (111) planes with a size between 4.9 and 7.4 nm, and then grow larger near the grain corner. The DTs were not observed in large grains because the DT nucleation requires very high stress.

Table I also shows that the critical stress for DT nucleation in nc Al is very high ( $>0.88$  GPa). It is very difficult, if not impossible, to reach such a high stress under normal, slow strain rate deformation. High strain rate and/or low temperature are known to promote the DT nucleation because they raise external stresses. This is consistent with experimental observations of DT in cryogenically ball-milled nc Al, which was subjected to both high strain rate and low temperature.<sup>7,15</sup> The high stress required for DT nucleation also explains the experimental observation that DT only appeared in a very small fraction of grains,<sup>7,15</sup> and does not play a major role in the deformation of nc Al. Note that another leading model<sup>18</sup> predicts a twin nucleation stress of 2 GPa, which is unlikely under the cryogenic ball milling conditions.

The current model predicts that the optimum grain size for DT nucleation in Cu is 38.4–54.2 nm. In the HPT-processed nc Cu, DTs were only observed in Cu grains smaller than 50 nm,<sup>28</sup> which is consistent with our model prediction. In addition, critical twinning stresses for Cu is 0.36–0.37 GPa (Table I), which can be easily reached under

the HPT condition, which were performed under a large compressive stress of 7 GPa. This also explains the high densities of twins in the HPT-processed nc Cu, which suggests that DT played a significant role in the deformation of nc Cu.

## C. Validity and limitation of the current model

In this model, we have made several assumptions to render the mathematics tractable without sacrificing physics. First we assumed a square grain shape and straight dislocation lines although real dislocations are curved. We also ignored the interaction between the dislocations and GBs. These assumptions make this model semiquantitative. However, we also note that the equation for dislocation line energy [Eq. (3)] from the classic dislocation theory is itself semiquantitative because of the uncertainty in determining the values of  $r_0$  and  $R$ . A recent MD simulation<sup>44</sup> shows that Eq. (3) is valid at grain sizes down to 2 nm, which validate our use of the equation at grain sizes relevant in the current model.

In this model, we do not consider dislocation nucleation from GBs, and assume that nongeometrically necessary dislocations already exist at GBs and can readily move under a sufficient external stress. Such type of dislocations are abundant in severe plastic deformation (SPD)-processed nc materials and such GBs have been termed nonequilibrium GBs.<sup>31,37</sup> Therefore, this model should work very well in nc materials synthesized by SPD techniques, which may be why it can explain well the experimental observations in cryogenic ball-milled Al (Refs. 15 and 16) and HPT-processed Cu.<sup>17,28</sup> For nc materials without nongeometrically necessary dislocations, e.g., nc materials synthesized by methods such as chemical-vapor deposition (CVD) and electrodeposition, dislocation nucleation is a critical step and deformation twinning would require higher external stresses than predicted by our current model. A model for dislocation nucleation from GBs would need to consider the generalized planar fault energies curves.<sup>36</sup>

## IV. CONCLUSIONS

We have further developed an earlier analytical-classical-dislocation-based model to describe DT nucleation. Simple analytical equations for calculating the critical twinning stress and optimum twinning grain size were developed for easy application of the model. Our model indicates that an optimum grain-size range exists in which the critical DT nucleation stress is the lowest. It also satisfactorily explains the experimental observations of DTs in both nc Al synthesized by cryogenic ball milling and nc Cu synthesized by HPT, attesting to its validity. Because the model does not address the dislocation nucleation from GBs, it may be applicable only in the nc fcc materials produced by SPD, in which nongeometrically necessary dislocations exist on the grain boundaries.

## ACKNOWLEDGMENTS

This work was supported by the US DOE IPP program office, the Office of Science and the ONR Grant No. N00014-04-1-0370.

- <sup>1</sup>S. X. McFadden, R. S. Mishra, R. Z. Valiev, A. P. Zhilyaev, and A. K. Mukherjee, *Nature (London)* **398**, 684 (1999).
- <sup>2</sup>R. Z. Valiev, I. V. Alexandrov, Y. T. Zhu, and T. C. Lowe, *J. Mater. Res.* **18**, 5 (2002).
- <sup>3</sup>K. S. Kumar, S. Suresh, M. F. Chisholm, J. A. Horton, and P. Wang, *Acta Mater.* **51**, 387 (2003).
- <sup>4</sup>D. Jia, Y. M. Wang, K. T. Ramesh, E. Ma, Y. T. Zhu, and R. Z. Valiev, *Appl. Phys. Lett.* **79**, 611 (2001).
- <sup>5</sup>X. Zhang, H. Wang, R. O. Scattergood, J. Narayan, C. C. Koch, A. V. Sergueeva, and A. K. Mukherjee, *Appl. Phys. Lett.* **81**, 823 (2002).
- <sup>6</sup>R. A. Masumura, P. M. Hazzledine, and C. S. Pande, *Acta Mater.* **46**, 4527 (1998).
- <sup>7</sup>X. Z. Liao, F. Zhou, E. J. Lavernia, S. G. Srinivasan, M. I. Baskes, D. W. He, and Y. T. Zhu, *Appl. Phys. Lett.* **83**, 632 (2003).
- <sup>8</sup>V. Yamakov, D. Wolf, S. R. Phillpot, A. K. Mukherjee, and H. Gleiter, *Nat. Mater.* **1**, 45 (2002).
- <sup>9</sup>J. Schiøtz, F. D. DiTolla, and K. W. Jacobsen, *Nature (London)* **391**, 561 (1998).
- <sup>10</sup>H. Van Swygenhoven, P. M. Derlet, and A. Hasnaoui, *Phys. Rev. B* **66**, 024101 (2002).
- <sup>11</sup>H. Van Swygenhoven, *Science* **296**, 66 (2002).
- <sup>12</sup>V. Yamakov, D. Wolf, S. R. Phillpot, and H. Gleiter, *Acta Mater.* **50**, 5005 (2002).
- <sup>13</sup>V. Yamakov, D. Wolf, S. R. Phillpot, A. K. Mukherjee, and H. Gleiter, *Nat. Mater.* **3**, 43 (2004).
- <sup>14</sup>J. Schiøtz and K. W. Jacobsen, *Science* **301**, 1357 (2003).
- <sup>15</sup>X. Z. Liao, F. Zhou, E. J. Lavernia, D. W. He, and Y. T. Zhu, *Appl. Phys. Lett.* **83**, 5062 (2003).
- <sup>16</sup>X. Z. Liao, S. G. Srinivasan, Y. H. Zhao, M. I. Baskes, Y. T. Zhu, F. Zhou, E. J. Lavernia, and H. F. Xu, *Appl. Phys. Lett.* **84**, 3564 (2004).
- <sup>17</sup>X. Z. Liao, Y. H. Zhao, S. G. Srinivasan, Y. T. Zhu, R. Z. Valiev, and D. V. Gunderov, *Appl. Phys. Lett.* **84**, 592 (2004).
- <sup>18</sup>M. Chen, E. Ma, K. J. Hemker, H. Sheng, Y. M. Wang, and X. Cheng, *Science* **300**, 1275 (2003).
- <sup>19</sup>H. Rösner, J. Markmann, and J. Weissmüller, *Philos. Mag. Lett.* **84**, 321 (2004).
- <sup>20</sup>R. C. Pond and L. M. F. Garcia-Gacia, *Inst. Phys. Conf. Ser.* **61**, 495 (1981).
- <sup>21</sup>C. D. Liu, M. N. Bassim, and D. X. You, *Acta Metall. Mater.* **42**, 3695 (1994).
- <sup>22</sup>N. Hansen and B. Ralph, *Acta Metall.* **30**, 411 (1982).
- <sup>23</sup>O. Johari and G. Thomas, *Acta Metall.* **2**, 1153 (1964).
- <sup>24</sup>C. S. Smith, *Trans. Metall. Soc. AIME* **212**, 574 (1958).
- <sup>25</sup>T. H. Blewitt, R. Coltman, and J. K. Redman, *J. Appl. Phys.* **28**, 651 (1957).
- <sup>26</sup>M. A. Meyers, O. Vöhringer, and V. A. Lubarda, *Acta Mater.* **49**, 4025 (2001).
- <sup>27</sup>E. El-Danaf, S. R. Kalidindi, and R. D. Doherty, *Metall. Mater. Trans. A* **30A**, 1223 (1999).
- <sup>28</sup>X. Z. Liao, Y. H. Zhao, Y. T. Zhu, R. Z. Valiev, and D. V. Gunderov, *J. Appl. Phys.* **96**, 636 (2004).
- <sup>29</sup>J. Wang and H. C. Huang, *Appl. Phys. Lett.* **85**, 5983 (2004).
- <sup>30</sup>A. G. Frøseth, H. Van Swygenhoven, and P. M. Derlet, *Acta Mater.* **52**, 2259 (2004).
- <sup>31</sup>X. Z. Liao, J. Y. Huang, Y. T. Zhu, F. Zhou, and E. J. Lavernia, *Philos. Mag.* **83**, 3065 (2003).
- <sup>32</sup>R. J. Asaro, P. Krysl, and B. Kad, *Philos. Mag. Lett.* **83**, 733 (2003).
- <sup>33</sup>Y. T. Zhu, X. Z. Liao, Y. H. Zhao, S. G. Srinivasan, F. Zhou, and E. J. Lavernia, *Appl. Phys. Lett.* **85**, 5049 (2004).
- <sup>34</sup>E. B. Tadmor and S. Hai, *J. Mech. Phys. Solids* **51**, 117 (2003).
- <sup>35</sup>J. R. Rice, *J. Mech. Phys. Solids* **40**, 239 (1992).
- <sup>36</sup>H. Van Swygenhoven, P. M. Derlet, and A. G. Frøseth, *Nat. Mater.* **3**, 399 (2004).
- <sup>37</sup>J. Y. Huang, Y. T. Zhu, H. Jiang, and T. C. Lowe, *Acta Mater.* **49**, 1497 (2001).
- <sup>38</sup>I. Kovács and L. Zsoldos, *Dislocation and Plastic Deformation* (Pergamon, Oxford, 1973), pp. 40–186.
- <sup>39</sup>J. P. Hirth and J. Lothe, *Theory of Dislocations* (Wiley, New York, 1982), p. 315 and 839.
- <sup>40</sup>E. A. Brades and G. B. Brook, *Smithell's Metal Reference Book*, 7th ed. (Butterworth-Heinemann, Oxford, 1992).
- <sup>41</sup>L. E. Murr, *Interfacial Phenomena in Metals and Alloys* (Addison-Wesley, London, 1975), p. 145.
- <sup>42</sup>V. Yamakov, D. Wolf, M. Salazar, S. R. Phillpot, and H. Gleiter, *Acta Mater.* **49**, 2713 (2001).
- <sup>43</sup>H. Van Swygenhoven, M. Spaczer, A. Caro, and D. Farkas, *Phys. Rev. B* **60**, 22 (1999).
- <sup>44</sup>C. H. Henager, Jr. and R. G. Hoagland, *Scr. Mater.* **50**, 1091 (2004).